AIMS Materials Science, 12(4): 728–743.
DOI: 10.3934/matersci.2025031
Received: 06 June 2025
Revised: 16 July 2025
Accepted: 25 July 2025
Published: 31 July 2025

http://www.aimspress.com/journal/Materials

Research article

Study on the influence of waste glass powder particle size and content on bond-slip performance of reinforced concrete

Shuisheng Yu[1,2,*], Junying Jing[1], Yi Zhao[1,2], Yuzhou Sun[2,3], Qingxiang Zhao[1] and Xin Li[1]

[1] School of Intelligent Construction and Civil Engineering, Zhongyuan University of Technology, Zhengzhou 450007, China
[2] Henan Engineering Research Center of Mechanics and Engineering Structures, Zhengzhou 450007, China
[3] Henan University of Urban Construction, Pingdingshan, 450007, China

* **Correspondence:** Email: yuss.1987@163.com.

Abstract: To investigate the influence of waste glass powder's particle size and content on the bond–slip behavior of reinforced concrete, this study integrates laboratory experiments with theoretical analysis to examine the effects of varying waste glass powder particle sizes (<20, 20–75, 75–150 μm) and replacement contents (10%, 20%, 30%) on bond–slip performance and failure modes. The research clarifies the mechanism by which waste glass powder affects bond–slip behavior and establishes a bond–slip constitutive model that accounts for the coupling effects of particle size and content. The results indicate that at the same replacement level, smaller waste glass powder particles exhibit a larger specific surface area and higher reactivity. This facilitates the formation of more calcium silicate hydrate gel through pozzolanic reactions, thereby enhancing concrete's compactness and bond strength. Under identical particle size conditions, bond strength first increases and then decreases with increasing waste glass powder content, peaking at a 10% replacement content. Compared with reference specimens without waste glass powder, this optimal replacement content enhances bond strength by 5.3%. An appropriate amount of waste glass powder can effectively fill concrete pores and improve the uniformity of stress distribution, with specimens exhibiting pull-out failure modes. However, excessive incorporation of waste glass powder may induce alkali–silica reactions, generating expansive gels that render concrete more prone to splitting failure. The proposed bond–slip model shows good agreement with the experimental results, accurately characterizing the bond–slip performance of waste glass powder-modified reinforced concrete under the combined influence of different particle sizes and replacement contents.

Keywords: reinforced concrete structure; waste glass powder; particle size; content; bond–slip model

1. Introduction

Societal development and rising economic standards have led to a dramatic surge in waste glass production. As a nonbiodegradable material, long-term landfilling of waste glass not only consumes substantial land resources but also exerts significant adverse impacts on the ecological environment. Thus, the recycling and disposal of waste glass have emerged as pressing environmental challenges requiring immediate attention. In the construction sector, appropriately processed waste glass can function as an alternative to cement [1]. Waste glass powder primarily consists of silicon dioxide (SiO_2) with small amounts of aluminum oxide (Al_2O_3). These components endow waste glass powder with high pozzolanic activity, enabling it to react with cement hydration products and form a gel with excellent binding properties—thereby improving the microstructure of concrete [2–4]. This denser microstructure can effectively enhance concrete's mechanical performance, resistance to chemical corrosion, and freeze–thaw durability [5–7]. As a result, the application of waste glass powder as a cement replacement admixture has garnered increasing research interest, offering substantial economic and environmental advantages.

In the study of concrete modified with waste glass powder, particle size distribution and content are key factors influencing concrete's performance. Consequently, researchers both domestically and internationally have carried out extensive investigations into the properties of waste glass concrete. Jiang et al. [8] used waste glass powder as a supplementary cementitious material for ordinary Portland cement (OPC). The results showed that the addition of waste glass powder improved the workability of OPC paste while prolonging the setting time. Waste glass powder could mitigate the degradation of the OPC matrix at high temperatures and reduce the alkali–silica reaction (ASR) effect. Research by Yu et al. [9] revealed that mortar containing undergoes a rapid decrease in both flexural and compressive strength during the initial erosion stage, followed by a slower decline in strength or even a recovery in strength when exposed to prolonged erosion. Tong et al. [10] suggested that while an optimal content of glass powder enhances the mechanical performance and durability of concrete, excessive amounts or larger particle sizes may exert detrimental effects. Studies by Peng et al. [11] and Rajendran et al. [12] demonstrated that incorporating 20% waste glass powder significantly improves the corrosion resistance and mechanical properties of recycled aggregate concrete; however, exceeding this optimal proportion leads to performance degradation and reduced workability. Shalan et al. [13] specifically examined the long-term sulfate resistance of concrete with varying waste glass powder contents, and compressive strength measurements confirmed that higher waste glass powder content notably enhances sulfate resistance. Jiang et al. [14] conducted research and found that adding waste glass powder can improve the fire resistance of fly ash-based polymer slurry. Furthermore, fluidity increases with the rise in waste glass powder content, and both compressive strength and bonding strength reach optimal levels when the waste glass powder content is 20%.

The incorporation of waste glass powder as a cement replacement significantly affects the performance of reinforced concrete structures, with both the replacement ratio and particle size playing crucial roles. Omer et al. [15] observed that under conditions of constant content, variations in waste glass particle size have a limited impact on the shear performance of beams, yet they can

substantially enhance cracking load, shear strength, and bending cracking load capacity. Yu et al. [16] demonstrated through bond performance tests that when the glass powder replacement ratio is 15%, the average bond strength between the reinforcement and concrete decreases as the replacement ratio increases; this downward trend is also observed when glass sand is used with replacement ratios up to 60%. Yassen et al. [17] revealed that although partial replacement of cement with waste glass powder increases the ultimate load capacity of beams, it simultaneously increases the material's brittleness, resulting in reduced vertical displacement in beams containing glass powder under the same loading conditions. Xiong et al. [18] found that compared with conventional reinforced concrete beams, those containing waste glass powder exhibit lower cracking loads. Moreover, as the content of waste glass powder increases, the bearing capacity gradually decreases while the mid-span deflection increases steadily.

In conclusion, waste glass powder demonstrates significant potential in enhancing the mechanical properties of concrete and improving the performance of reinforced concrete structures. However, there are still relatively few studies on the impact of waste glass powder on the bond performance of reinforced concrete. Therefore, the purpose of this research was to explore the effects of different particle sizes and contents of waste glass powder on the bond performance of reinforced concrete. The influence laws of different waste glass powder conditions on the bond strength, sliding characteristics, and failure mode of reinforced concrete were studied, and a concrete bond–sliding constitutive model with the interactive effect of waste glass powder particle size and content was established, providing a theoretical basis for the application of waste glass powder in engineering structures.

2. Materials and methods

2.1. Specimen materials and preparation

The experimental materials used in this study consisted of the following. The cement adopted is OPC with a compressive strength of 42.5 MPa. Three different particle size ranges of waste glass powder, namely below 20 μm (D1), 20–75 μm (D2), and 75–150 μm (D3), were adopted. The main chemical composition of the waste glass powder is shown in Table 1. The fine aggregate was natural river sand with a particle size distribution of 0.3–2.36 mm. The coarse aggregate was pebbles with a particle size distribution of 5–20 mm. The water used was tap water. The proportions of waste glass powder replacing cement with the same mass were 10%, 20%, and 30%, denoted as R10, R20, and R30 respectively. The specimens are marked as D1R10, D2R20, and D3R10, etc. For example, the label D1R10 indicates that the specimens are concrete with a particle size of less than 20 μm and a waste glass powder content of 10%. The mix ratios of waste glass powder and concrete with different particle sizes are all shown in Table 2 [19].

Table 1. Main chemical components of waste glass powder.

Analyte	SiO_2	Na_2O	CaO	Al_2O_3	MgO	K_2O	Fe_2O_3
wt (%)	67.21	13.57	7.23	3.73	2.16	1.98	0.96

Table 2. Mix ratios of waste glass powder and concrete [19].

Content of waste glass powder (%)	Cement	Sand	Waste glass powder	Stone	Water
0	1	1.3	0	3.02	0.47
10	0.9	1.3	0.1	3.02	0.47
20	0.8	1.3	0.2	3.02	0.47
30	0.7	1.3	0.3	3.02	0.47

The concrete specimens used in the test were cylindrical, with a diameter of 150 mm and a height of 75 mm. The reinforcing bars adopted are HRB400 grade reinforcing bars with a diameter of 12 mm and a length of 200 mm, and the anchoring length of the reinforcing bars is 75 mm. The specific dimensional parameters of the specimens are shown in Figure 1.

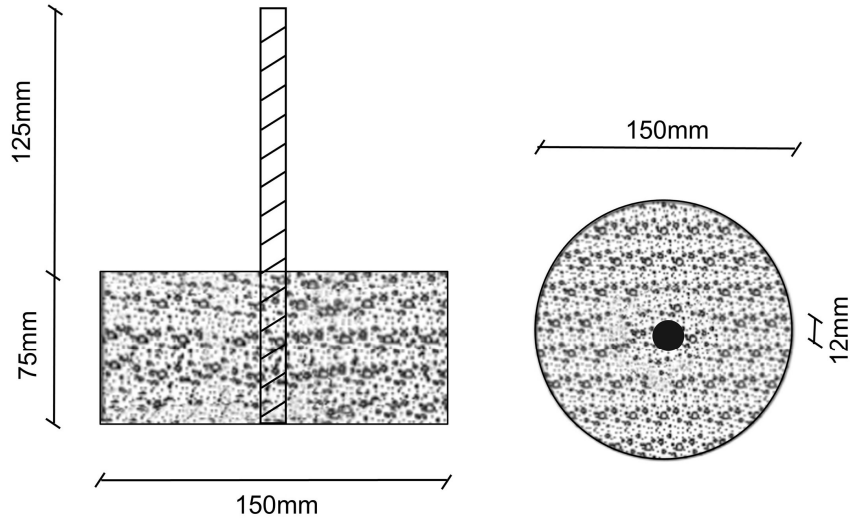

Figure 1. Specimens' size parameters.

The method for making the test piece is as follows. The HRB400 grade reinforcing bar with a diameter of 12 mm is centered and positioned through the holes on the top and bottom gaskets, ensuring that the bar remains in the center of the specimen. Then the proportionally mixed concrete is poured, and the mold is placed on the vibration table for vibration. A steel wire is used to stir the mixture to ensure that the concrete is fully compacted and internal air bubbles are expelled. After the pouring is completed, the specimen is left to stand for 24 h. Once the concrete has initially hardened, the mold is removed, and the specimen is placed in a standard curing room for continuous curing for 28 days. After the curing is completed, a center pull-out test is conducted on the specimen to test the bond–slip performance between the reinforcing bar and the concrete. Three parallel specimens were set for each group, and the final result is the average of the tests.

2.2. Test method

The pull-out test was conducted using the WAW-600C electro-hydraulic servo universal testing machine. The slip of the reinforcing bars was measured by a displacement gauge installed at the

bottom of the specimen, and the load was measured by a pressure sensor at the bottom of the specimen. All the test data during the test process were automatically collected by a data acquisition system. Before loading the test, we ensured that the test bench was clean and aligned the centerline of the reinforcing bars with the loading end of the testing machine in a straight line to prevent the reinforcing bars from being pulled unevenly. During the test, a displacement control loading method with a loading rate of 0.5 mm/min was adopted, and the loading was continued until the specimen failed. The test loading device is shown in Figure 2.

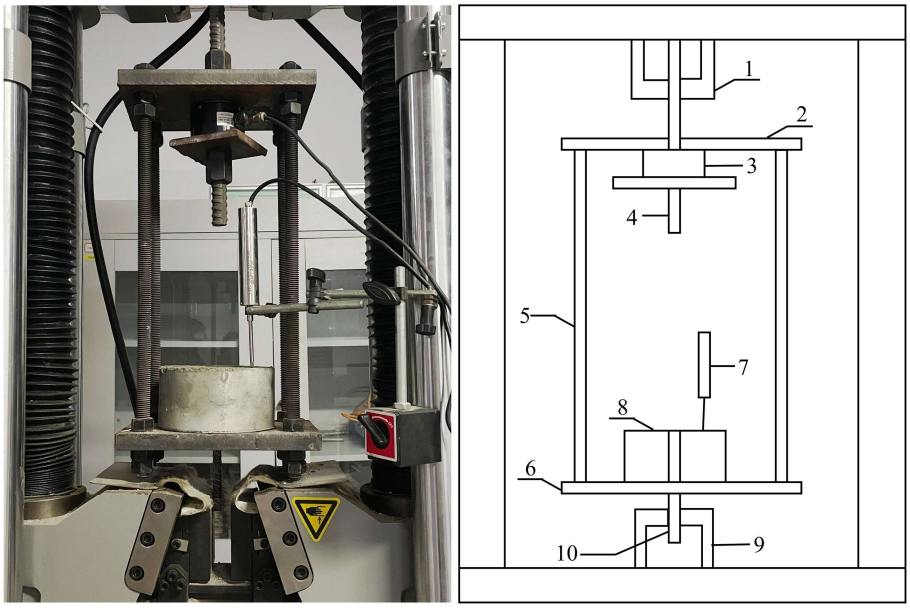

Figure 2. Test device. 1: Installation fixture; 2: upper steel plate; 3: pressure sensor; 4: steel tie rods; 5: steel support rods; 6: lower steel plate; 7: displacement meter; 8: concrete; 9: lower fixture; 10: reinforcing bars.

Assuming that the bonding stress is uniformly distributed along the reinforcing bars, and taking the average bonding strength between the reinforcing bars and the waste glass powder concrete as the maximum bonding stress within the anchorage length of the reinforcing bars, the calculation formula for bonding strength is given by Eq 1:

$$\tau = \frac{F}{\pi DL} \tag{1}$$

where τ is the mean bonding stress, F is the pull-out load, D represents the diameter of the reinforcing bars, and L represents the anchoring length of the reinforcing bars.

3. Experimental results and analysis

3.1. The effect of different particle sizes on the bond–slip behavior of reinforced concrete

Figure 3 illustrates the effect of different particle sizes of waste glass powder on the bond–slip behavior of reinforced concrete under identical admixture conditions. The experimental results show a progressive decrease in bond strength and a significant increase in slip displacement as the particle

size increases from below 20 to 150 μm. This behavior stems from the higher specific surface area and enhanced pozzolanic activity of finer waste glass powder, which facilitates more complete secondary hydration reactions with calcium hydroxide in cement hydration products, producing abundant dense calcium silicate hydrate gel. Zhao et al. [20] confirmed through scanning electron microscopy (SEM) analysis that this calcium silicate hydrate gel effectively fills the concrete matrix's pores and seals cracks in the interfacial transition zone, reducing both crack density and width while improving zone densification. Conversely, coarser waste glass powder exhibits a reduced specific surface area and lower reactivity, leading to limited participation in hydration reactions and consequently minimal improvements in pore-filling and mechanical properties, explaining the observed strength reduction with increasing particle size. Additionally, Li et al. [21] demonstrated that larger waste glass particles more readily initiate alkali–silica reactions, producing expansive gels that further degrade interfacial bonding. The particle size increase weakens the interfacial bond between glass particles and the cement matrix, creating additional microcracks and pore defects in the transition zone that act as stress-induced slip channels, resulting in greater peak slip displacements with larger particles.

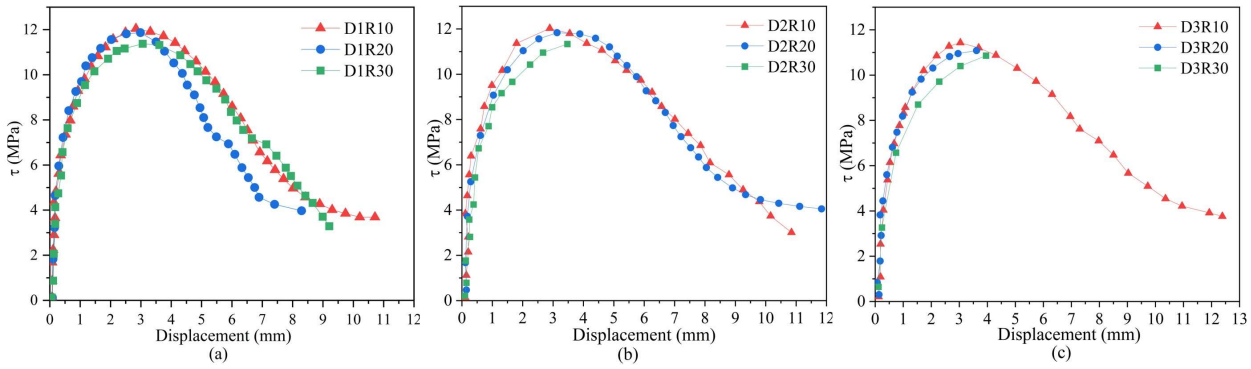

Figure 3. Influence of different particle sizes on the bond–slip behavior of reinforced concrete: (a) R10; (b) R20; (c) R30.

Figure 4 illustrates the relationship between bond stress–slip displacement and particle size in reinforced concrete with varying waste glass powder contents. The results reveal that under equivalent replacement contents, bond strength exhibits a distinct inverse correlation with particle size, while peak slip displacement shows a positive correlation. The most significant performance improvement is observed when using waste glass powder with a particle size below 20 μm at a 10% replacement content, achieving a 5.3% increase in bond strength. This enhancement is attributed to the material's larger specific surface area, which promotes more thorough pozzolanic reactions. Furthermore, specimens incorporating this finer particle size exhibit 8.1–17.9% lower peak slip displacements compared with those with larger particles. This confirms that the calcium silicate hydrate gel formed significantly improves the microstructure of the interfacial transition zone and effectively inhibits both the initiation and propagation of cracks.

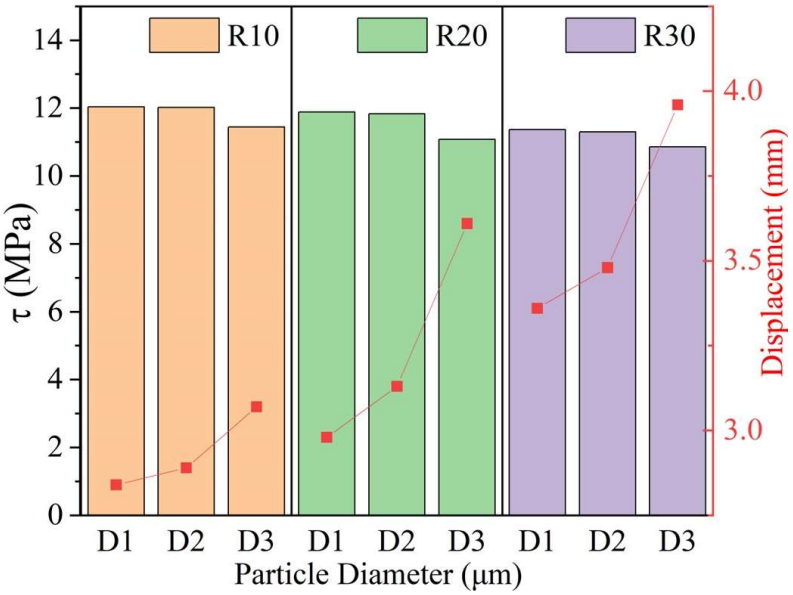

Figure 4. Relationship between bond stress–slip displacement and waste glass powder content with different particle sizes in reinforced concrete.

3.2. The effect of varying proportions of waste glass powder on the bond–slip behavior of reinforced concrete

Figure 5 demonstrates the influence of waste glass powder content on the bond–slip behavior of reinforced concrete with constant particle size. Test results reveal that when the waste glass powder content rises from 10% to 30%, the bond strength progressively declines while the peak slip displacement shows marked growth. This behavior occurs because at 10% content, the waste glass powder optimally fills the matrix's pores, enhances cement hydration, and produces calcium silicate hydrate gel through pozzolanic reactions, thereby improving the concrete's density and bond performance. At 20% content, a moderate bond strength reduction appears, since the waste glass powder starts partially inhibiting cement hydration, causing slight deterioration in the cement paste's microstructural compactness. When the content reaches 30%, bond strength suffers a substantial reduction because excessive waste glass powder cannot completely participate in hydration, leaving numerous unreacted particles that weaken the interfacial transition zone's mechanical properties. With increasing content, these unreacted particles accumulate in the transition zone, creating porous weak areas that diminish interfacial friction and mechanical interlocking while inducing internal structural loosening, consequently leading to significantly greater peak slip displacements at higher contents.

Figure 6 illustrates the relationship between bond stress–slip displacement and waste glass powder content in reinforced concrete with different waste glass powder particle sizes. The results indicate that under identical particle size conditions, bond strength decreases nonlinearly as the waste glass powder content increases, while peak slip displacement shows a positive correlation with content. For all waste glass powder particle sizes, the optimal performance is achieved at a 10% content, with bond strength increasing by 5.3%, 5.1%, and 0.1%, respectively, for 10%, 20%, and 30%. Moreover, at this content, the peak slip displacement is 18.3–30% lower compared with specimens with higher replacement contents (20% and 30%).

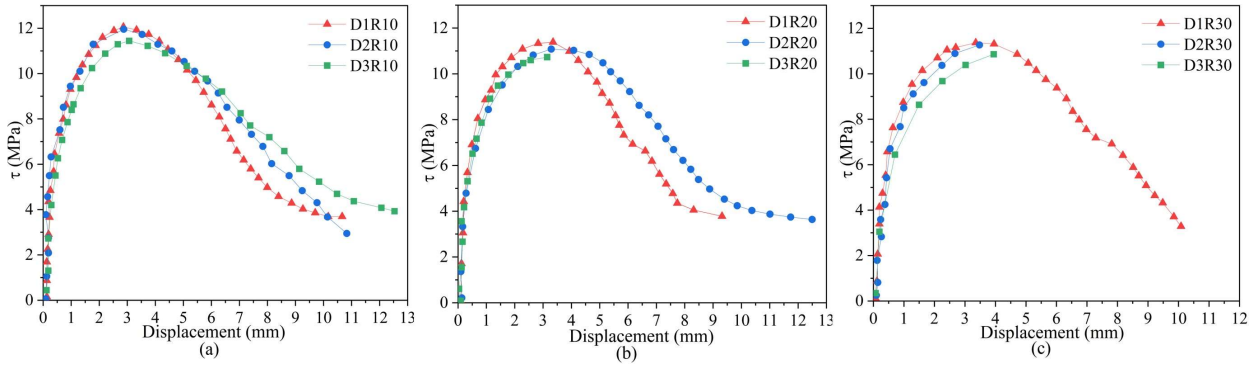

Figure 5. Influence of different waste glass powder contents on the bond–slip behavior of reinforced concrete: (a) D1; (b) D2; (c) D3.

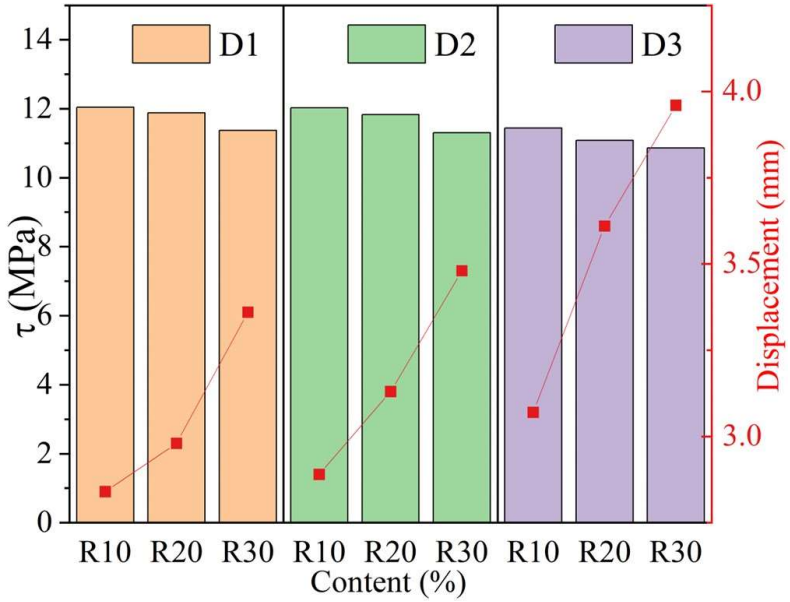

Figure 6. Relationship between bond stress–slip displacement and waste glass powder content at different particle sizes in reinforced concrete.

3.3. The failure mechanism of reinforced concrete with waste glass powder

The incorporation of waste glass powder in concrete initiates two crucial chemical reactions. The alkali–silica reaction occurs when the alkaline components in concrete chemically interact with waste glass powder to produce alkali–silicate gel. This hygroscopic gel expands upon water absorption, generating internal stresses that may cause concrete cracking and structural deterioration, as represented by Eq 2. Conversely, the pozzolanic reaction involves waste glass powder reacting with cement hydration products to form calcium silicate hydrate gel. This reaction not only improves concrete's strength but also effectively inhibits the formation of expansive alkali–silica gel, with its chemical process detailed in Eq 3.

$$SiO_2 + 2Na^+(K^+) + 2OH^- \longrightarrow Na_2(K_2)SiO_3H_2O \quad (2)$$

$$SiO_2 + Ca^{2+} + 2OH^- \longrightarrow n_1\mathrm{CaO} \cdot SiO_2 \cdot n_2H_2O \quad (3)$$

The incorporation of waste glass powder in concrete, considering both its content and particle size, is closely related to the failure modes of reinforced concrete specimens, primarily manifested in splitting failure and pull-out failure. When a high content of waste glass powder or when coarse particle sizes are used, the specimens tend to experience splitting failure, as shown in Figure 7a. The failure of the reinforced concrete specimen is accompanied by a clear brittle fracture sound, with cracks initially forming at the free end of the specimen and rapidly extending toward the loading end. This is because, during the pull-out process, radial stress develops at the interface between the steel reinforcement and the concrete due to the bond stress. When the concrete's hoop tensile strength is insufficient to resist this radial stress, longitudinal splitting occurs. Moreover, the incorporation of larger waste glass particles may induce alkali–silica reactions, producing expansive reaction gels that generate supplementary tensile stresses within the concrete matrix, thereby significantly accelerating crack propagation rates and exacerbating structural damage.

When specimens incorporate moderate amounts of fine-grained waste glass powder, they typically exhibit pull-out failure characteristics, as illustrated in Figure 7b. These specimens show minimal surface cracking, often with only a few fine cracks or even no visible cracks at all. The failure process involves a gradual increase in bond stress until reaching the maximum, followed by controlled extraction of the steel bar. This improved performance arises from the microfilling effect of waste glass powder: Its fine particles optimize the pore structure of the cement matrix, reduce the brittleness of concrete, and enhance the mechanical properties of the interfacial transition zone. These microstructural enhancements promote a more uniform stress distribution across the specimen, effectively preventing crack formation induced by localized stress concentrations.

(a) (b)

Figure 7. Failure modes of specimens: (a) splitting failure; (b) pull-out damage.

4. Bond–slip model of waste glass powder-reinforced concrete

In the study of bond–slip constitutive relationships for reinforced concrete, traditional models such as the Malvar model, the Eligehause–Popov–Bertero model (BPE model), modified BPE model, and Cosenza–Manfredi–Realfonzo model (CMR model) [22–25], although capable of describing bond–slip behavior to varying extents, fail to simultaneously satisfy the requirements for smooth continuity and the clear physical concepts of the bond–slip curve. Therefore, on the basis of

comprehensive experimental investigations and theoretical analyses, Gao et al. [26] developed a novel continuous curve model to characterize the constitutive relationship of bond–slip in reinforced concrete, as illustrated in Figure 8. This advanced model accurately captures the bond–slip behavior in three distinct phases. (1) The initial loading phase demonstrates a near-linear stress–slip relationship dominated by chemical adhesion and frictional forces. (2) Upon reaching peak stress, chemical bonds fail while microcracks initiate, propagate, and coalesce within the concrete matrix, leading to progressive stress reduction. (3) Beyond a critical slip threshold, the bond stress tends to stabilize, mainly through the friction and partial residual interlocking forces between the steel ribs and the concrete, maintaining residual load-bearing capacity. The corresponding constitutive equation for reinforced concrete's bond–slip behavior is presented in Eq 4.

$$\begin{cases} \dfrac{\tau}{\tau_{\mathrm{u}}} = 2\sqrt{\dfrac{s}{s_u}} - \dfrac{s}{s_u} & 0 \le s \le s_u \\ \tau = \tau_{\mathrm{u}} \dfrac{(s_r - s)^2(2s + s_r - 3s_u)}{(s_r - s_u)^3} + \tau_r \dfrac{(s - s_u)^2(3s_r - 2s - s_u)}{(s_r - s_u)^3} & s_u \le s \le s_r \end{cases} \tag{4}$$

Where τ_u and S_u represent the peak bond strength and the corresponding slip, and τ_r and S_r represent the bond strength and the corresponding slip in the residual phase.

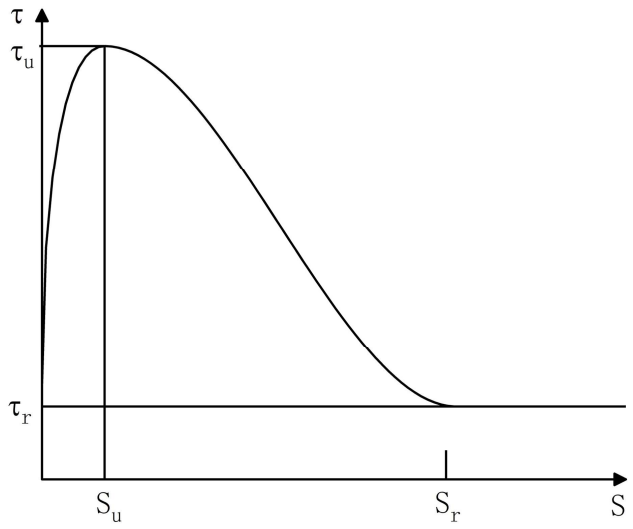

Figure 8. Continuous curve model.

In order to further study the influence of the particle size and content of waste glass powder on the bond–slip performance of reinforced concrete, the continuous curve model was modified. Since the mechanical behavior in the residual stage is mainly dominated by the friction between the ribs on the surface of the reinforcing bars and the concrete aggregates, and has a relatively weak correlation with the pozzolanic activity or particle size effect of the waste glass powder. Therefore, in this paper, only the influence coefficients of the particle size and content of the waste glass powder on the bond strength and peak slip are introduced, as expressed in Eq 5.

$$\begin{aligned} \tau_{dr} &= \tau_0 \times \gamma \times \omega \\ s_{dr} &= s_0 \times \alpha \times \beta \end{aligned} \tag{5}$$

Where τ_{dr} and s_{dr} represent the bond strength and peak slip corresponding to different particle sizes and contents of waste glass powder, τ_0 and s_0 represent the bond strength and peak slip for the concrete without waste glass powder, γ and ω represent the effects of particle size and content on bond strength, and α and β represent the effects of particle size and content on peak slip.

The continuous curve model proposed by Gao et al. [26] was modified to develop a bond–slip model for waste glass powder-reinforced concrete under the synergistic effects of varying waste glass powder particle sizes and contents, as shown in Eq 6.

$$\tau = \begin{cases} \tau_{\mathrm{dr}} \times \left(2\sqrt{\dfrac{s_{\mathrm{dr}}}{s_u}} - \dfrac{s_{\mathrm{dr}}}{s_u} \right) & (0 < s_{\mathrm{dr}} \le s_u) \\ \tau_{\mathrm{dr}} \dfrac{(s_r - s_{\mathrm{dr}})^2 (2s_{\mathrm{dr}} + s_r - 3s_u)}{(s_r - s_u)^3} + \tau_r \dfrac{(s_{\mathrm{dr}} - s_u)^2 (3s_r - 2s_{\mathrm{dr}} - s_u)}{(s_r - s_u)^3} & (s_u < s_{\mathrm{dr}} \le s_r) \\ \tau_r & (s_{\mathrm{dr}} > s_r) \end{cases} \tag{6}$$

Figures 9 and 10 show the bond strength ratio and peak slip ratio of reinforced concrete under the synergistic effects of waste glass powder's particle size and content. Here, τ_d represents the bond strength of reinforced concrete under the effect of particle size, τ_d/τ_0 represents the bond strength ratio under the effect of particle size, τ_r represents the bond strength of reinforced concrete under the effect of content, τ_r/τ_0 represents the bond strength ratio under the effect of content, S_d represents the peak slip of reinforced concrete under the effect of particle size, S_d/S_0 represents the peak slip ratio under the effect of particle size, S_r represents the peak slip of reinforced concrete under the effect of content, and S_r/S_0 represents the peak slip ratio under the effect of content.

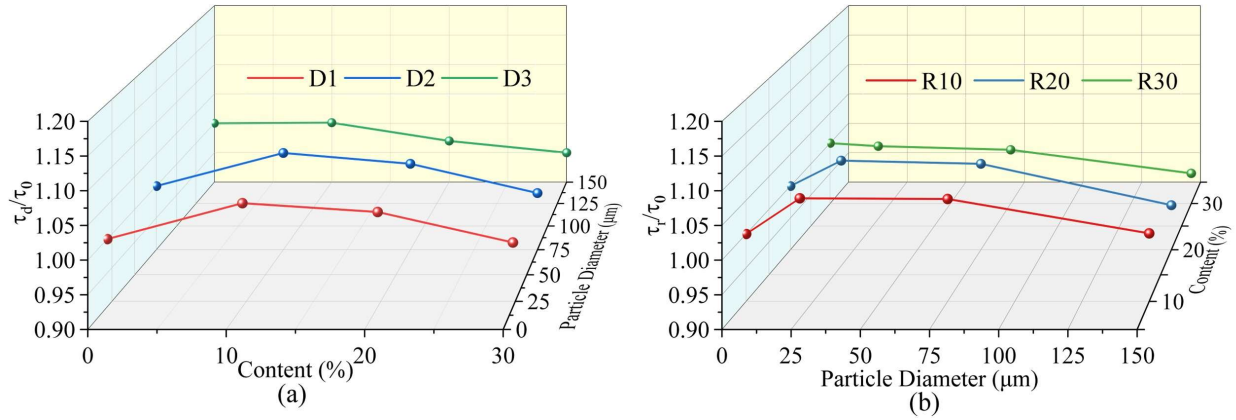

Figure 9. Bond strength ratio under different waste glass powder parameters: (a) different particle sizes; (b) different contents.

Figure 9 reveals that the optimal enhancement of bond strength is achieved when using waste glass powder with a D1 particle size at 10% content. This optimal performance arises from the combined benefits of the powder's microaggregate filling effect and retained pozzolanic activity, which significantly improves the microstructure of the interfacial transition zone. However, when the particle size exceeds D1 or the content surpasses 10%, all particle size groups exhibit a notable reduction in the bond strength ratio. This deterioration occurs because larger particles, with their reduced specific surface area, have diminished pozzolanic reactivity; meanwhile, excessive content leads to the accumulation of unreacted particles in the interfacial zone, impairing the mechanical

properties of the transition zone. In contrast, Figure 10 shows that the peak slip ratio follows the opposite trend, increasing with both particle size and content. The D3 particle size group at a 30% content reaches a maximum slip ratio of 1.4. This is attributed to weakened particle–matrix interlocking and the accumulation of unreacted particles at the interface, which create microcracks and pore defects, ultimately forming a continuous weak zone with enhanced deformation capacity.

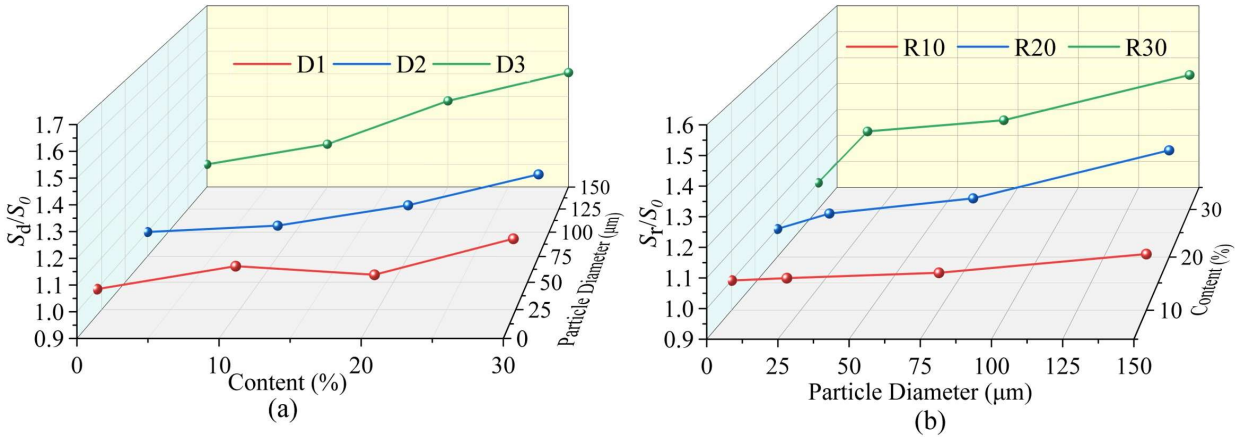

Figure 10. Peak slip ratio under different waste glass powder parameters: (a) different particle sizes; (b) different contents.

The fitting analysis of the results in Figures 9 and 10 reveals the effects of different waste glass powder particle sizes and contents on bond strength, represented by the parameters γ and ω, as well as the effects on peak slip, represented by the parameters α and β. The fitting result is shown in Eqs 7–10:

$$\gamma = \begin{cases} -2.45*10^{-4}d^2+0.007d+1.002 & d \le 20 \\ -2.725*10^{-4}d^2+0.008d+1.004 & 20 \le d \le 75 \\ -0.525*10^{-4}d^2-2.35*10^{-4}d+1 & 75 \le d \le 150 \end{cases} \quad (7)$$

$$\omega = \begin{cases} -0.977*10^{-5}r^2+0.001r+1.011 & r \le 10 \\ -0.933*10^{-5}r^2+0.001r+1.008 & 10 \le r \le 20 \\ -0.239*10^{-5}r^2+3.921*10^{-5}r+1 & 20 \le r \le 30 \end{cases} \quad (8)$$

$$\alpha = \begin{cases} 0.006*e^{0.119d}+0.992 & d \le 20 \\ 0.043*e^{0.063d}+0.954 & 20 \le d \le 75 \\ 1.031*e^{0.011d}-0.04 & 75 \le d \le 150 \end{cases} \quad (9)$$

$$\beta = \begin{cases} 0.017*e^{0.012r}+0.984 & r \le 10 \\ -190.9*e^{-9.3*10^{-6}r}+191.9 & 10 \le r \le 20 \\ -0.425*e^{-0.012r}+1.462 & 20 \le r \le 30 \end{cases} \quad (10)$$

To thoroughly verify the accuracy of the bond–slip model for waste glass powder-reinforced concrete structures, three representative test specimens (D1R10, D2R20, D3R10) were selected for validation analysis of the constitutive model. As shown in Figure 11, the bond–slip relationship exhibits three distinct phases. (1) The ascending phase demonstrates a linear or near-linear increase in bond strength with slip displacement. (2) The descending phase shows a gradual reduction in bond strength with continued slip displacement at the loading end. (3) The residual phase features

stabilized bond strength at reduced levels, indicating structural failure. As shown in Figure 11, the differences between the model's results and the experimental data mainly occur in the residual stage. Since the bond–slip model only considers the influence of particle size and content on the bonding performance, it does not fully account for the physical and chemical effects of the waste glass powder in the interface transition zone during the residual stage, resulting in a deviation between the constant assumption of friction and the actual situation. However, the error between the test results and the model results is within an acceptable range, verifying the validity of the bond–slip model for waste glass powder-reinforced concrete structures under the combined effect of particle size and content.

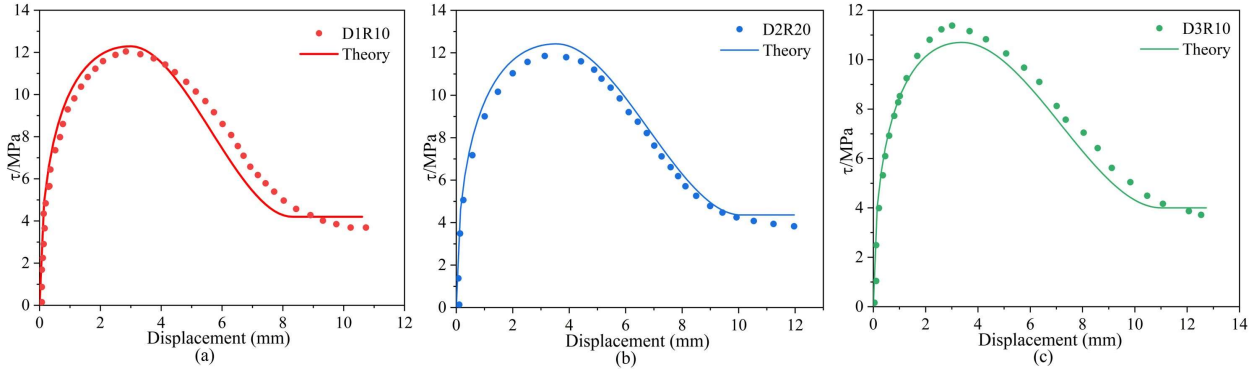

Figure 11. Comparison between theoretical models and experimental results: (a) D1R10; (b) D2R20; (c) D3R10.

5. Conclusions

This paper, by combining indoor experiments and theoretical analysis, studied the influence of different particle sizes and contents of waste glass powder on the bond–slip performance of reinforced concrete. On the basis of the experimental results, the following conclusions can be drawn.

(1) Under identical replacement content conditions, increasing the particle size of waste glass powder reduces its specific surface area and reactivity, consequently decreasing the quantity of calcium silicate hydrate gel produced through pozzolanic reactions. This results in progressively diminished concrete density and bond strength. Conversely, with a constant particle size, bond strength demonstrates an initial increase followed by a decrease as the waste glass powder content rises, peaking at 10% content with a 5.3% enhancement compared with reference specimens without waste glass powder.

(2) The failure mode of waste glass powder-reinforced concrete exhibits significant dependence on both the particle size and content parameters. When utilizing larger particle sizes, the material tends to initiate alkali–silica reactions that produce expansive gel products, generating substantial internal swelling pressures within the concrete matrix. This expansive action results in markedly increased crack propagation, consequently transforming the failure mechanism from predominant reinforcement pull-out failure to concrete splitting failure.

(3) The developed bond–slip constitutive model for waste glass powder-reinforced concrete successfully characterizes the interfacial bond behavior across varying particle size distributions and replacement contents, demonstrating good agreement with experimental observations.

Use of AI tools declaration

The authors declare they have not used Artificial Intelligence (AI) tools in the creation of this article.

Acknowledgments

This work is funded by the International Science and Technology Cooperation project of Henan Province (241111521200), the Young Backbone Teacher of Zhongyuan University of Technology (2023XQG13), and Discipline Youth Master's Supervisor Training Program of Zhongyuan University of Technology (SD202424). This support is gratefully acknowledged.

Author contributions

Shuisheng Yu: writing-original draft, funding acquisition, conceptualization; Junying Jing: writing-review & editing, visualization; Yi Zhao: project administration, methodology; Yuzhou Sun: validation, formal analysis; Qingxiang Zhao: supervision; Xin Li: investigation.

Conflicts of interest

The authors declare no conflict of interest.

References

1. Nodehi M, Mohamad Taghvaee V (2022) Sustainable concrete for circular economy: A review on use of waste glass. *Glass Struct Eng* 7: 3–22. https://doi.org/10.1007/s40940-021-00155-9
2. Li S, Jiang Y, Zhou J (2025) Fracture resistance of UHPC-CA with amorphous silica: Competition between microstructure densification and shrinkage microcracking. *Theor Appl Fract Mec* 138: 104886. https://doi.org/10.1016/j.tafmec.2025.104886
3. Zhao H, Li W, Gan Y, et al. (2023) Nano/microcharacterization and image analysis on bonding behaviour of ITZs in recycled concrete enhanced with waste glass powder. *Constr Build Mater* 392: 131904. https://doi.org/10.1016/j.conbuildmat.2023.131904
4. Zhan P, Zhang X, He Z, et al. (2022) Strength, microstructure and nanomechanical properties of recycled aggregate concrete containing waste glass powder and steel slag powder. *J Clean Prod* 341: 130892. https://doi.org/10.1016/j.jclepro.2022.130892
5. Tahwia AM, Essam A, Tayeh BA, et al. (2022) Enhancing sustainability of ultra-high performance concrete utilizing high-volume waste glass powder. *Case Stud Constr Mat* 17: e01648. https://doi.org/10.1016/j.cscm.2022.e01648
6. Dalila C, Mebarek B (2022) Effect of recycled waste glass addition on the resistance of high performance concrete to freeze-thaw cycles. *Jordan J Civ Eng* 16: 254–265. https://doi.org/10.1007/s40940-021-00155-9
7. Li C (2024) Study on compressive strength and sulfate corrosion resistance of limestone powder and waste glass powder mixed concrete. *Mater Res Express* 11: 025502. https://doi.org/10.1088/2053-1591/ad1ef6

8. Jiang X, Xiao R, Bai Y, et al. (2022) Influence of waste glass powder as a supplementary cementitious material (SCM) on physical and mechanical properties of cement paste under high temperatures. *J Clean Prod* 340: 130778. https://doi.org/10.1016/j.jclepro.2022.130778
9. Yu Z, Wen B, Wang H (2025) Study on the bonding properties of dual-substitution waste glass concrete with steel bars. *Constr Build Mater* 473: 140999. https://doi.org/10.1016/j.conbuildmat.2025.140999
10. Tong G, Pang J, Shen J, et al. (2024) Response tests on the effects of particle size of waste glass sand and glass powder on the mechanical and durability performance of concrete. *Sci Rep* 14: 25445. https://doi.org/10.1038/s41598-024-76164-9
11. Peng L, Zhao Y, Ban J, et al. (2023) Enhancing the corrosion resistance of recycled aggregate concrete by incorporating waste glass powder. *Cement Concrete Comp* 137: 104909. https://doi.org/10.1016/j.cemconcomp.2022.104909
12. Rajendran R, Sathishkumar A, Perumal K, et al. (2021) An experiment on concrete replacing binding material as waste glass powder. *Mater Today Proc* 47: 5447–5450. https://doi.org/10.1016/j.matpr.2021.06.431
13. Shalan AH, El-Gohary MM (2022) Long-term sulfate resistance of blended cement concrete with waste glass powder. *Pract Period Struct* 27: 04022047. https://doi.org/10.1061/(ASCE)SC.1943-5576.0000731
14. Jiang X, Xiao R, Ma Y, et al. (2020) Influence of waste glass powder on the physico-mechanical properties and microstructures of fly ash-based geopolymer paste after exposure to high temperatures. *Constr Build Mater* 262: 120579. https://doi.org/10.1016/j.conbuildmat.2020.120579
15. Omer B, Saeed J (2024) Evaluating the shear performance of reinforced concrete beams using waste glass powder as a sustainable cement substitute. *Struct Concrete* 25: 4812–4832. https://doi.org/10.1002/suco.202301002
16. Yu S, Wu S, Zhao Y, et al. (2023) Experimental study of sulfate erosion resistance of cementitious sand with waste glass powder. *Buildings* 13: 2037. https://doi.org/10.3390/buildings13082037
17. Yassen MM, Hama SM, Mahmoud AS (2023) Shear behavior of reinforced concrete beams incorporating waste glass powder as partial replacement of cement. *Eur J Environ Civ En* 27: 2194–2209. https://doi.org/10.1080/19648189.2022.2114946
18. Xiong W, Gan Y, Ke G, et al. (2017) Experimental study on shear behavior of waste glass powder reinforced concrete beams. *Concrete* 4: 65–68 (in Chinese). https://doi.org/10.3969/j.issn.1002-3550.2017.04.016
19. Yu S, Zhu W, Niu Li et al. (2019) Experimental and numerical analysis of fully-grouted long rockbolt load-transfer behavior. *Tunn Undergr Sp Tech* 85: 56–66. https://doi.org/10.1016/j.tust.2018.12.001
20. Zhao Y, Chen S, Yu S, et al. (2025) Study on the mechanical properties and microstructure of PVA fiber-reinforced waste glass powder concrete. *AIP Adv* 15: 015124. https://doi.org/10.1063/5.0244985
21. Li F, Yang J, Li L (2022) Effect and mechanism of waste glass powder as supplementary cementitious material on mortar properties. *BCCS* 41: 3208–3218 (in Chinese). Available from: https://www.opticsjournal.net/Articles/OJa5c17f65e58c38de/References.

22. Malvar LJ (1994) *Bond Stress-Slip Characteristics of FRP Rebars*, Port Hueneme, California: Naval Facilities Engineering Service Center.
23. Eligehausen R, Popov EP, Bertero VV (1983) Local bond stress-slip relationships of deformed bars under generalized exci-tations: Experimental results and analytical mode. *EERC* 69–80. http://dx.doi.org/10.18419/opus-8473
24. Cosenza E, Manfredi G, Realfonzo R (1995) Analytical modelling of bond between FRP reinforcing bars and concrete. Non-Metallic (FRP) Reinforcement for Concrete Structures—Proceedings of the Second International RILEM Symposium (FRPRCS-2), Ghent, Belgium ,164–171.
25. Cosenza E, Manfredi G, Realfonzo R (1997) Behavior and modeling of bond of FRP rebars to concrete. *J Compos Constr* 1: 40–51. https://doi.org/10.1061/(ASCE)1090-0268(1997)1:2(40)
26. Gao D, Zhu H, Xie J (2003) Bond-slip constitutive model of fiber reinforced plastic reinforced concrete. *Ind Constr* 33: 41–43 (in Chinese). https://doi.org/10.3321/j.issn:1000-8993.2003.07.011